Astronomy Letters, Vol. 25, No. 7, 1999, pp. 453–466. Translated from Pis'ma v Astronomicheskii Zhurnal, Vol. 25, No. 7, 1999, pp. 530–544.

Atmospheric Chemical Composition of the "Twin" Components of Equal Mass in the CP SB2 System 66 Eri

A. V. Yushchenko[1], V. F. Gopka[1], V. L. Khokhlova[2], F. A. Musaev[3], and I. F. Bikmaev[4]

[1] *Astronomical Observatory, Odessa State University, Shevchenko Park, Odessa, 270014 Ukraine*

[2] *Institute of Astronomy, Russian Academy of Sciences, Pyatnitskaya ul. 48, Moscow, 109017 Russia*

[3] *Special Astrophysical Observatory, Russian Academy of Sciences, Nizhni Arkhyz, Stavropol krai, 357147 Russia*

[4] *Kazan State University, ul. Lenina 18, Kazan, 420008 Tatarstan, Russia*

Received December 2, 1998

Abstract—We determine the atmospheric chemical composition of the components of the CP SB2 system 66 Eri with approximately equal masses ($M_A/M_B = 0.97$) by using two CCD echelle spectra of the star. These spectra have been taken with the 1-m telescope at Special Astrophysical Observatory with a spectral resolution of 36000 and a signal-to-noise ratio no less than 100 in the wavelength range 4385–6695 Å. The model-atmosphere parameters for the components are estimated by analyzing all available photometric and spectrophotometric data and the equivalent widths of iron lines. For components A and B, we have obtained $T_{\mathrm{eff}_A} = 11100$ K, $T_{\mathrm{eff}_B} = 10900$ K, $\log g_A = 4.25$, $\log g_B = 4.25$, $V_{\mathrm{turb}_A} = 0.9$ km s^{-1}, $V_{\mathrm{turb}_B} = 0.7$ km s^{-1}, and $v \sin i_{A,B} = 17$ km s^{-1}. The derived projected rotational velocities of the components, together with the HIPPARCOS parallax and photometric observations, show that their rotation may be synchronized with the orbital period. The star exhibits a considerable infrared excess at wavelengths longer than 25 μm. The synthetic-spectrum and model-atmosphere methods are used to determine the atmospheric abundances of 26 chemical elements in component B and 15 chemical elements in component A. The components differ markedly in chemical composition. The peculiar component B exhibits no chemical anomalies that are typical of the Hg–Mn group, such as an underabundance of He and Al and an enhancement of P and Ga, but shows large heavy-element overabundances reaching 4–5 dex. The atmosphere of component A also exhibits moderate overabundances of Mn and Ba, but no lines of other heavy elements have been found in its spectrum. However, an estimate of the upper limit on their abundances does no rule out small heavy-element overabundances in the atmosphere of component A either. 66 Eri is the first and the only close SB2 system with CP non-Hg–Mn components studied to date.

INTRODUCTION

This study is part of our program of atmospheric-abundance analysis for SB2 systems whose components have equal masses and are unevolved main-sequence stars. Such stars can be arbitrarily called twins because they are similar in physical parameters, initial chemical composition, and age. The component–mass ratio for 66 Eri (HD 32964), $M_A/M_B = 0.97$ (Young 1976), is closest to unity among the stars of this program studied to date: AR Aur (Khokhlova *et al.* 1995) and 46 Dra (Tsymbal *et al.* 1998). The components are of the same spectral type: B9.5 V + B9.5 Vp (Batten *et al.* 1989).

The spectroscopic orbital parameters of 66 Eri were analyzed by Frost and Struve (1924) and Young (1976). The latter author noted that the components of 66 Eri were almost identical in all physical characteristics, except the atmospheric chemical composition. Based on photographic spectra with a dispersion of 13 Å mm^{-1}, Young identified absorption lines of Fe, Ti, Ni, Si, Sr, Ca, and Mg in the spectra of both components and absorption lines of Y, Cr, and Hg only in the spectrum of component B. This author attempted to observe an eclipse in the system but found no light variations. On this basis, Young estimated the orbital inclination to be $i < 80°$.

Below, we give the orbital elements from Young (1976):

$$P = 5.522731 \text{ days}$$

$$e = 0.095$$

$$V_0 = +32.6 \pm 0.8 \text{ km s}^{-1}$$

$$T_0 = 2441384.13 \pm 0.1$$

$$K_A = 103.8 \pm 1.3 \text{ km s}^{-1}$$

$$K_B = 107.7 \pm 0.7 \text{ km s}^{-1}$$

$$a_A \sin i = (7.85 \pm 0.10) \times 10^6 \text{ km}$$

$$a_B \sin i = (7.61 \pm 0.06) \times 10^6 \text{ km}$$

$$M_A \sin^3 i = 2.38 \pm 0.05 M_\odot$$

1063-7737/99/2507-0453$15.00 © 1999 МАИК "Наука/Interperiodica"

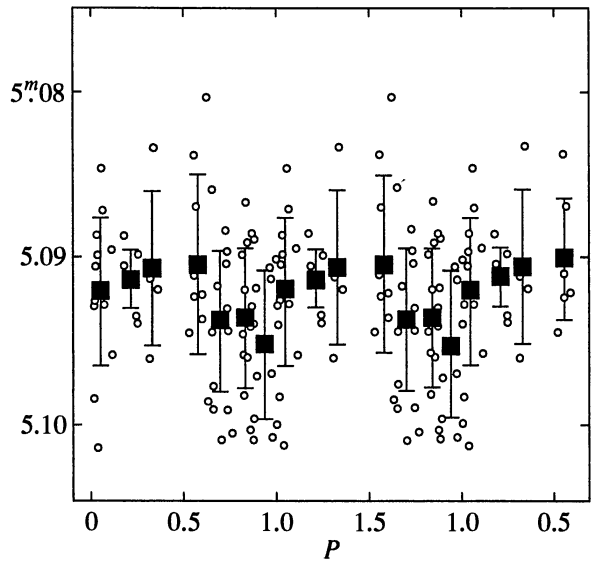

Fig. 1. Light curve of 66 Eri (EN Eri) as constructed from the Hipparcos observations. The period was assumed to be equal to half the orbital period. The circles and squares denote individual observations and mean data points. The rms errors of the mean data points are indicated by the vertical bars.

$$M_B \sin^3 i = 2.45 \pm 0.05 M_\odot.$$

Schneider (1987) carried out photometric observations in the Strömgren system and reported a very small variability (with an amplitude of $0^m.002$ in v and $0^m.005$ in u) with a period of 7.8586 days. In the General Catalog of Variable Stars, 66 Eri is listed as the variable EN Eri, which belongs to the α^2CVn stars.

Berghofer and Schmidt (1994), who studied the X-ray emission from late B-type stars by using data from the ROSAT all-sky survey, found 66 Eri (along with 46 Dra) to be an X-ray source. The observations of 66 Eri during the flights of several astronomical satellites have yielded photometric and spectrophotometric data in the wavelength range 0.134 to 100 μm. Preliminary results of the abundance analysis for 66 Eri were published in part by Yushchenko *et al.* (1998).

Table 1. Measured radial velocities of 66 Eri

JD_{hel}	Phase	Component	V_r, km s^{-1}	N	σ, km s^{-1}
2450057.375	0.647	A	123.1	13	0.7
		B	–53.0	18	0.3
2450060.406	0.196	A	–74.8	20	0.5
		B	142.9	13	0.7

SPECTROSCOPIC OBSERVATIONS

We used the spectra of 66 Eri that were obtained at two orbital phases with the echelle spectrometer attached to the 1-m Special Astrophysical Observatory telescope. The spectrometer was described by Musaev (1996). The spectra were taken on a 580 × 530-pixel CCD array with a spectral resolution $R = 36\,000$ in the wavelength range 4385–6695 Å and a signal-to-noise ratio no less than 100.

For the initial reduction of echelle images and spectra and for wavelength calibration, we used a modified version (1996) of the DECH20 software package (Galazutdinov 1992), which was provided by the author. The further reduction of the spectra was performed by using the URAN (Yushchenko 1998) and STARSP (Tsymbal 1996) software packages.

We drew the continuum using the synthetic spectrum of the binary system that we computed by adding up the synthetic spectra of the components shifted in accordance with their observed radial velocities. The observed data were smoothed with a Gaussian filter with the FWHM equal to half the width of the instrumental profile. The equivalent widths of spectral lines were determined by fitting a Gaussian to the observed line profile.

HIPPARCOS PHOTOMETRIC OBSERVATIONS

To analyze the photometric variability of 66 Eri, we used the Hipparcos photometry (Perryman *et al.* 1997): 74 magnitude estimates for the star in the interval JD 2447910–2449061. In most cases, the measurement errors were $0^m.004$–$0^m.005$. The periodograms of these observations were analyzed by means of the Fourier transform of discontinuous observational series (Deeming 1975) and by the method of Andronov (1994). We searched for periodicities in the interval from 100 to 0.5 days. The strongest peaks in the power spectrum were interpreted as combinations of the peaks corresponding to the peaks in the power spectrum of the spectral window (attributable to periodicity in the distribution of epochs of observations) and a 2.761365-day period, which is equal to half the orbital period of the spectroscopic binary.

After subtracting the mean light curve corresponding to the 2.761365-day period, we repeated the search for periodicities. Since the accuracy of the observations was relatively low, we could not distinguish any period in the residual power spectrum. Note that the primary and secondary power spectra exhibit no significant peaks near the 7.86-day period that was found by Schneider (1987). Figure 1 shows the light curve of 66 Eri as constructed from the Hipparcos observations with the elements

$$\mathrm{Min}_{hel} = 2441383.112 + 2.761365E.$$

The initial epoch was taken from Young (1976). These results cannot be reliably interpreted due to the

Table 2. Photometric and spectrophotometric data and physical parameters of 66 Eri

Photometric system or satellite	Reference to catalog	Wavelengths (μm)	Reference to calibration	Colors	T_{eff}	log g
uvbs spectrophotometry	Jamar *et al.* (1976)	0.136–0.274				
ANS	Wesselius *et al.* (1982)	0.155–0.33				
TD1	Thompson *et al.* (1978)	0.156–0.274				
UBVRI	Lanz (1986)	0.36–0.79	Kurucz (1993)	*B–V*, *U–B*	10950	4.25
uvby	Hauck and Mermilliod (1990)	0.35–0.55	Smalley (1996)		11100	4.3
			Stepien (1994)		10540	
Geneva	Rufener (1988)	0.35–0.58	Kunzli *et al.* (1997)		11070	4.25
JHKL	Gezari *et al.* (1993)	1.25–3.4	Dougherty *et al.* (1993)	*V–J*	11170	
	Gezari *et al.* (1996)			*V–H*	10950	
IRAS	Moshir *et al.* (1989)	12–100		*V–L*	10860	

measurement errors which are comparable to the amplitude of the light curve. Further high-accuracy photometric observations of 66 Eri are required.

RADIAL VELOCITIES

To measure the radial velocities of the components of 66 Eri, we selected unblended lines of ionized iron with equivalent widths no less than 10 mÅ. We used the method of spectrum decomposition into Gaussians (Kasatella 1975), which allows the wavelengths of spectral lines to be determined with a high accuracy. The measured radial velocities were averaged with weights inversely proportional to the width of the spectral order containing the line under study. Table 1 gives the heliocentric Julian dates of the observations, the corresponding orbital phases (according to the ephemeris of Young 1976), designations for the binary components for which the measurements were made, the mean radial velocities, the number of measured spectral lines, and the errors of the weighted mean.

ATMOSPHERIC PHYSICAL PARAMETERS OF THE COMPONENTS OF 66 ERI

Since the components of 66 Eri are very similar in their physical characteristics, we were able to use photometric calibrations for single stars to determine their mean parameters. The distance to 66 Eri is ~100 pc, and the color excess $E(B–V)$ does not exceed $0^m.02$. The low interstellar extinction toward 66 Eri allowed us to obtain reliable values of the effective temperature and surface gravity from the photometric and spectrophotometric data listed in Table 2.

This table also gives references to the photometric calibrations we used and the mean effective temperatures and surface gravities that we determined by assuming solar metallicity for 66 Eri. As we see from the table, most values of the effective temperature lie in the range 10780 to 11 170 K. The mean surface gravity of the components as estimated from the photometric data is close to $\log g = 4.25$.

The photometric and spectrophotometric observations of 66 Eri in the wavelength range 0.134 to 100 μm (see Table 2) allowed us to construct the spectral energy distribution of the binary system and to compare it with

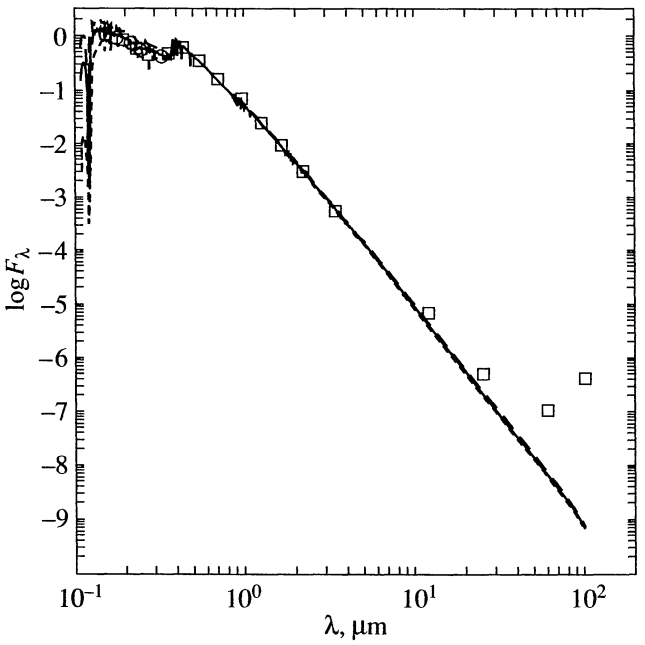

Fig. 2. Comparison of the spectral energy distribution for 66 Eri with theoretical fluxes. The circles and squares represent observations, and the lines represent computed fluxes. See the text for a description.

computed energy distributions. Figure 2 compares the spectral energy distribution of 66 Eri with three theoretical energy distributions which were computed by Kurucz (1993) for models with effective temperatures of 10000, 11000, and 12000 K. For all three models, we assumed $\log g = 4.5$, a microturbulent velocity of 2 km s^{-1}, and solar metallicity. As we see from Fig. 2, the spectrum of 66 Eri at wavelengths longer than 25 μm exhibits a large infrared excess reaching two orders of magnitude.

Figure 3 represents the left part of Fig. 2—the ultraviolet, visible, and near-infrared ranges—on an enlarged scale. Apart from the energy distributions computed with the above Kurucz's models, Fig. 3 shows the energy distribution that we computed for a model atmosphere from Kurucz's (1993) grid of models for solar metallicity with $T_{\rm eff} = 11000$ K, $\log g = 4$, and a microturbulent velocity of 2 km s^{-1}. We took the elemental abundances from our preliminary abundance determinations for the secondary component of 66 Eri.

According to these determinations, the abundances of light elements and some of the iron-group elements are nearly solar. The abundances of Cr, Mn, Co, Ni, and heavy elements relative to the Sun increase with atomic number; for mercury, the overabundance reaches 5 dex. In our calculations, we used the line list from the LOWLINES.DAT file (Kurucz 1993), which contains more than 30 million spectral lines, and a modified version of the code for computing synthetic spectra by Tsymbal (1994). All computed values of the energy distribution were reduced to the observed flux from 66 Eri at 0.55 μm: 0.335×10^{-10} erg s^{-1} cm^{-2} $Å^{-1}$. The unity of the y-axis in Figs. 2 and 3 corresponds to 10^{-10} erg s^{-1} cm^{-2} $Å^{-1}$.

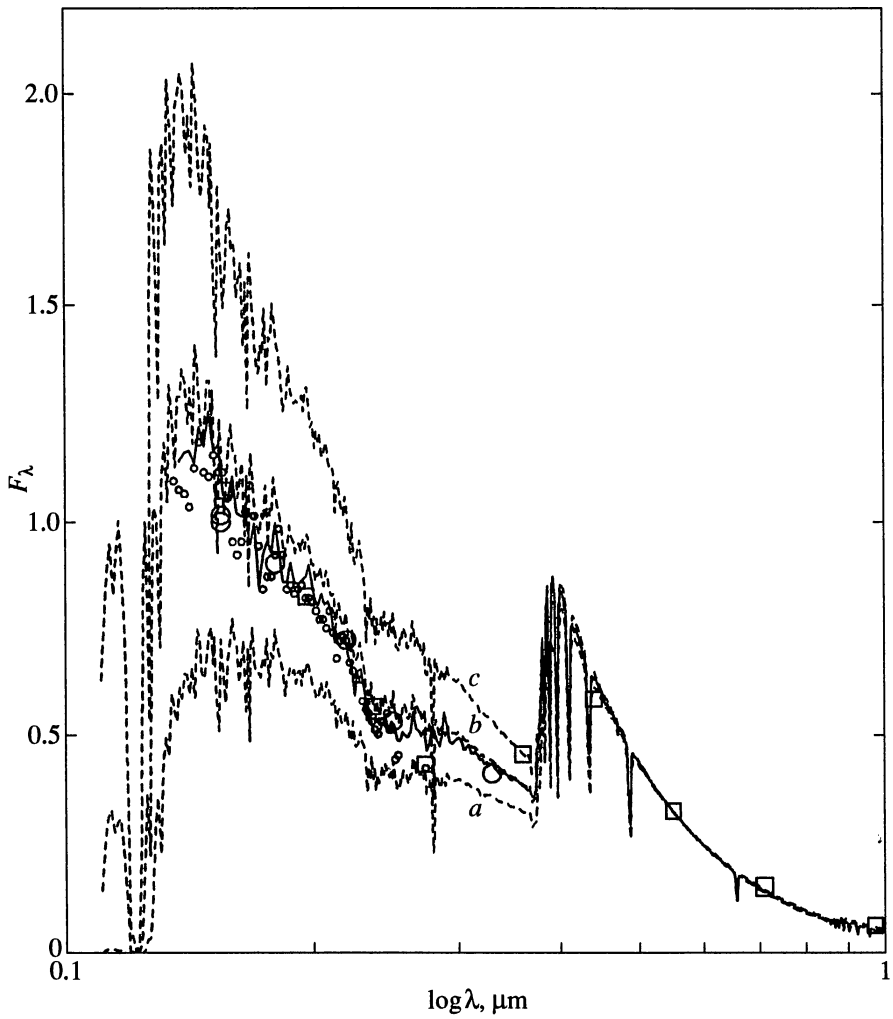

Fig. 3. Comparison of the spectral energy distribution for 66 Eri with theoretical fluxes for wavelengths shorter than 1μm. The small circles denote *uvbs* spectrophotometry, and the large circles and squares denote photometry. The dashed lines represent the calculations of Kurucz (1993) for models with solar metallicity, $\log g = 4.5$, and temperatures of 10000, 11000, and 12000 K. The solid line represents our calculations with a temperature of 11000 K and the chemical composition of the anomalous component B which we derived in the first approximation.

It follows from Fig. 3 that, when the energy distributions computed with solar chemical composition are used, the mean temperature of the binary system 66 Eri is close to 10800 K. A comparison of our calculations for anomalous chemical composition with the calculations for solar chemical composition leads us to conclude that an enhancement of heavy elements results in a higher effective temperature.

Having analyzed the photometric and spectrophotometric data, we found that the mean temperature of the components of 66 Eri was close to 11000 K and that the surface gravity was close to $\log g = 4.25$. These parameters can be used to determine the chemical composition if the components are identical.

Nevertheless, we made an attempt to find a difference between the components by using spectroscopic data. For this purpose, we selected unblended lines of singly ionized iron in the spectra of both components (these lines are listed in Table 3), adopted the previously derived surface gravity $\log g = 4.25$ for the two components, and attempted to determine the effective temperature and microturbulent velocity for each component separately and their luminosity ratio.

We used a grid of model atmospheres with $T_{\rm eff}$ from 10700 to 11300 K at steps of 100 K and a microturbulent velocity from 0.2 to 1.3 km s^{-1} at steps of 0.1 km s^{-1}.

The model atmospheres were selected or interpolated from Kurucz's (1993) grid of stellar model atmospheres with solar metallicity and a microturbulent velocity of 1 km s^{-1}. The calculations for each model were performed with correction factors of the equivalent widths for binarity from 1.7 to 2.3 at steps of 0.025. Since the spectral types of the components are similar, we ignored the wavelength dependence of these factors.

For each model and for each correction factor of the equivalent widths for binarity, we determined the iron abundance from FeII lines for the two components using two spectra. For each grid point, we computed the following:

(1) the correlation coefficient between the equivalent widths of the FeII lines and the iron abundances derived from these lines;

(2) the correlation coefficient between the energies of the lower level for the FeII lines and the iron abundances derived from these lines;

(3) the rms error of the mean iron abundance.

An analysis of the calculations allowed us to select grid points for which the above correlation coefficients were close to zero and, simultaneously, the rms error of the mean iron abundance was at a minimum.

We thus obtained the following temperatures and microturbulent velocities for the components of 66 Eri and their luminosity ratio:

component A:

$T_{\rm eff_A} = 11100 \pm 100$ K, $V_{\rm turb_A} = 0.9 \pm 0.2$ km s^{-1};

component B:

$T_{\rm eff_B} = 10900 \pm 100$ K, $V_{\rm turb_B} = 0.7 \pm 0.2$ km s^{-1},

luminosity ratio $L_A/L_B = 0.95 \pm 0.05$.

This procedure for determining the component parameters also automatically yields the iron abundance in each star. We did not use the condition of ionization equilibrium to determine the surface gravity in the atmosphere of each star, because the measured lines of neutral iron in the spectrum of 66 Eri were few and weak.

The derived atmospheric parameters of the components were used to compute the hydrogen-line profiles in the spectrum of 66 Eri. Extracting the observed hydrogen-line profiles from echelle spectra requires special tricks, because both line wings do not fit into one order, and the profile has to be joined. Figure 4 shows that the observed and computed profiles are in reasonably good agreement.

SYNCHRONIZATION OF ROTATION OF 66 ERI

When the synchronization of rotation with orbital motion of the components of 66 Eri is considered, several contradictions arise. The measured widths of metal lines allowed the projected rotational velocities of the two components to be estimated: $v \sin i = 17$ km s^{-1}.

Despite the large scatter of data points and the small amplitude, the Hipparcos photometric data (Fig. 1) suggest a possible variability with the period equal to half the orbital period, i.e., the possible detection of eclipses (essentially contacts) of the stellar disks. We can thus determine the orbital inclination, $i_{\rm orb} = 81°$. If the rotation of the components and their orbital motion are coaxial and synchronized, which is typical of such systems, then we obtain $1.72 R_\odot$ for the radii.

On the other hand, the Hipparcos parallax of 66 Eri is 11.65 ± 0.73 mas. Knowing the parallax, the apparent magnitude $v = 5^m.12$, the bolometric correction BC = $-0^m.57$ (Kurucz 1993), the flux ratio, and the effective temperatures of the components, we can determine the component radii, $R_A = 1.75 R_\odot$ and $R_B = 1.86 R_\odot$, which are in good agreement with those obtained above from the synchronization condition. The derived radii and surface gravities allow the component masses to be estimated, $M_A = 2.0 M_\odot$ and $M_B = 2.2 M_\odot$, in good agreement with $M \sin^3 i$ from Young (1976).

However, the component radii determined in this case, $R = 1.72 R_\odot$, turn out to be appreciably smaller than the radii of main-sequence stars with $T_{\rm eff} = 11000$ K, for which Allen (1977) obtained $R = 2.8 R_\odot$.

An alternative possibility can be based on the Tycho parallax (8.3 ± 0.73 mas), which yields $R_A = 2.45 R_\odot$ and $R_B = 2.61 R_\odot$. In this case, either there is synchronization but no coaxiality (the inclination of the rotation axes with respect to the line of sight is i rot = 44°) or

Table 3. List of lines used to determine the atmospheric parameters of the components of 66 Eri and the elemental abundances

λ, Å	Ion	Equivalent width, mA				log*N* (log*N*(H) = 12.00)				log*gf*	*Ei*
		component A		component B		component A		component B			
		1	2	1	2	1	2	1	2		
4471.473	HeI*	48	–	–	45	10.90	–	–	10.93	–.28	20.963
4713.139	HeI*	14	–	12	–	10.99	–	11.00	–	–1.23	20.963
5875.615	HeI*	31	35	28	28	10.97	11.02	10.96	11.02	.41	20.963
6678.154	HeI*	8	12	–	9	10.85	11.13	–	10.99	.33	21.217
5052.167	CI*	3.5	–	4.5	–	8.40	–	8.37	–	–1.65	7.684
5330.741	OI*	19	16	20	17	8.77	8.79	8.67	–	–1.12	10.740
5436.862	OI*	8	–	–	–	8.78	–	–	–	–1.51	10.740
6155.971	OI*	10	18	15	20	8.77	8.83	8.68	8.69	–1.05	10.740
6156.755	OI*	22	25	22	20	8.77	8.83	8.68	8.69	–.93	10.740
6158.187	OI*	25	30	27	30	8.77	8.83	8.68	8.69	–.44	10.740
6402.246	NeI*	3	–	–	–	8.15	–	–	–	.36	16.618
4702.991	MgI*	10	12	6	8	7.42	7.50	7.19	7.18	–.67	4.346
5167.322	MgI*	23	23	8	15	7.63	7.52	7.03	7.2	–1.03	2.70
5172.684	MgI*	30	–	20	23	7.42	–	–	7.12	–.40	2.711
5183.604	MgI*	–	40	–	–	–	7.44	–	–	–.18	2.716
4390.572	MgII*	30	25	–	–	7.40	7.41	–	–	–.53	9.999
4427.994	MgII*	–	13	–	15	–	7.36	–	7.23	–1.21	9.995
4433.988	MgII*	–	20	22	24	–	7.33	7.17	7.17	–.91	9.999
4481.136	MgII*	165	168	145	158	7.78	7.68	7.34	7.50	.74	8.863
4663.046	AlII*	14	15	8	–	6.53	6.58	6.21	–	–.28	10.598
5593.300	AlII*	–	4	–	–	–	6.72	–	–	.41	13.256
6231.750	AlII*	–	6	–	4	–	6.73	–	6.42	.40	13.072
5041.024	SiII*	3	33	37	32	6.91	6.82	6.85	6.77	.29	10.066
5055.984	SiII*	4	52	48	53	6.98	6.81	6.83	6.98	.59	10.073
5978.930	SiII*	2	23	–	21	7.22	7.27	–	6.92	.00	10.073
6371.371	SiII*	0	–	–	–	6.75	–	–	–	.00	8.121
4815.552	SII	5	–	–	–	7.47	–	–	–	.18	13.671
5453.855	SII*	4	–	4	–	7.21	–	7.28	–	.56	13.671
4716.743	CaII	4	–	3	–	6.46	–	6.24	–	–.94	7.047
5019.971	CaII	–	10	7	–	–	6.53	6.24	–	–.26	7.514
5031.021	ScII	3.5	–	–	–	3.35	–	–	–	–.26	1.357
5526.790	ScII	–	–	4	–	–	–	3.14	–	.13	1.768
4394.051	TiII	–	–	13	16	–	–	5.57	5.72	–1.78	1.221
4395.033	TiII	34	30	43	46	5.40	5.17	5.80	5.98	–.51	1.084
4399.772	TiII	10	11	29	29	5.01	5.06	5.83	5.83	–1.27	1.237
4417.719	TiII	14	–	–	32	5.34	–	–	6.12	–1.43	1.165
4443.794	TiII	25	26	40	43	5.09	5.14	5.82	5.98	–.70	1.080
4450.482	TiII	14	13	27	28	5.32	5.27	5.83	5.8	–1.45	1.08
4488.331	TiII	–	11	21	–	–	5.63	6.03	–	–.82	3.123
4501.273	TiII	24	24	38	42	5.11	5.11	5.77	5.99	–.75	1.116

Table 3. (Contd.)

λ, Å	Ion	Equivalent width, mA				log*N* (log*N*(H) = 12.00)				log*gf*	*Ei*
		component A		component B		component A		component B			
		1	2	1	2	1	2	1	2		
4529.474	TiII	4.5	–	15	16	5.14	–	5.73	6.78	–1.65	1.572
4533.969	TiII	32	–	42	–	5.38	–	5.85	–	–.54	1.237
4563.761	TiI	19	19	38	35	5.14	5.14	6.03	5.86	–.96	1.221
4571.968	TiII	25	30	40	42	5.19	5.45	5.89	6.00	–.53	1.572
4589.958	TiII	–	7	21	–	–	5.15	5.80	–	–1.62	1.237
4911.193	TiII	5	–	24	21	5.02	–	6.01	5.86	–.65	3.123
5226.543	TiII	–	–	–	25	–	–	–	5.85	–1.30	1.566
5336.771	TiII	–	4	16	15	–	5.13	5.83	5.79	–1.70	1.582
5208.419	CrI	–	–	4.5	–	–	–	6.09	–	.16	.941
4554.988	CrII	13	14	25	–	5.82	5.88	6.38	–	–1.28	4.071
4558.650	CrII	27	–	–	33	5.72	–	–	6.00	–.45	4.073
4588.199	CrII	28	–	34	–	5.96	–	6.24	–	–.63	4.071
4565.740	CrII	–	–	–	13	–	–	–	6.30	–1.82	4.042
4588.199	CrII	–	22	–	38	–	5.63	–	6.47	–.63	4.071
4592.049	CrII	–	10	24	–	–	5.59	6.27	–	–1.22	4.073
4616.629	CrII	10	11	25	25	5.67	5.72	6.39	6.39	–1.29	4.072
4618.803	CrII	21	21	31	32	5.80	5.77	6.28	6.33	–0.84	4.073
4634.070	CrII	18	15	27	–	5.79	5.64	6.20	–	–0.99	4.072
4812.337	CrII	–	6	14	14	–	5.94	6.40	6.40	–1.96	3.864
5237.329	CrII	–	20	–	34	–	6.03	–	6.71	–1.09	4.073
5274.964	CrII	9	17	22	–	5.62	6.07	6.27	–	–1.29	4.071
5313.563	CrII	–	10	–	22	–	5.87	–	6.45	–1.47	4.073
5502.067	CrII	5	7	11	–	6.06	6.24	6.46	–	–1.99	4.168
5508.606	CrII	4	–	7	–	6.06	–	6.30	–	–2.11	4.156
4755.727	MnII	–	5	–	11	–	5.81	–	6.23	–1.24	5.397
4764.728	MnII	–	8	–	17	–	6.19	–	6.67	–1.35	5.398
4755.727	MnII	–	–	12	–	–	–	6.29	–	–1.24	5.397
4404.750	FeI	19	–	13	16	7.72	–	7.27	7.43	–.14	1.557
4528.613	FeI	4	–	3.5	3.5	7.74	–	7.54	7.55	–0.82	2.176
4920.502	FeI	–	11	–	–	–	7.77	–	–	.06	2.832
4957.597	FeI	–	–	–	14	–	–	–	7.73	.13	2.808
4982.524	FeI	–	4.5	–	–	–	7.85	–	–	.14	4.103
5125.112	FeI	2	–	–	–	7.81	–	–	–	–.14	4.220
5162.292	FeI	–	–	2.5	–	–	–	7.61	–	.02	4.177
5232.939	FeI	7	–	–	–	7.82	–	–	–	–.19	2.940
5269.537	FeI	–	–	–	7	–	–	–	7.69	–1.32	.859
5369.958	FeI	–	–	–	4	–	–	–	7.63	.35	4.371
5383.369	FeI	–	7	–	–	–	7.85	–	–	.50	4.312
4416.830	FeII	26	–	28	27	7.65	–	7.71	7.65	–2.60	2.778
4451.551	FeII	11	–	12	–	7.79	–	7.83	–	–1.84	6.138
4489.183	FeII	18	21	20	21	7.63	7.78	7.69	7.73	–2.97	2.828
4493.529	FeII	4	–	–	–	7.65	–	–	–	–1.43	7.919

Table 3. (Contd.)

λ, Å	Ion	Equivalent width, mA				log*N* (log*N*(H) = 12.00)				log*gf*	*Ei*
		component A		component B		component A		component B			
		1	2	1	2	1	2	1	2		
4515.339	FeII	31	27	33	28	7.88	7.63	7.93	7.63	–2.48	2.844
4520.224	FeII	–	29	27	25	–	7.84	7.68	7.57	–2.60	2.806
4541.524	FeII	21	19	19	–	7.88	7.77	7.72	–	–3.05	2.855
4555.893	FeII	–	32	30	31	–	7.73	7.55	7.60	–2.29	2.828
4576.340	FeII	15	16	15	17	7.55	7.61	7.50	7.61	–3.04	2.844
4580.063	FeII	–	–	7	–	–	–	7.55	–	–3.72	2.583
4583.837	FeII	35	35	38	37	7.60	7.60	7.71	7.65	–2.02	2.806
4620.521	FeII	12	13	12	12	7.62	7.67	7.57	7.57	–3.28	2.828
4629.339	FeII	28	–	34	31	7.57	–	7.86	7.67	–2.37	2.806
4635.316	FeII	–	14	12	–	–	7.71	7.57	–	–1.65	5.956
4666.758	FeII	11	–	12	–	7.61	–	7.62	–	–3.33	2.828
4948.793	FeII	–	6	–	5	–	7.69	–	7.58	–.01	10.347
4951.584	FeII	7	–	–	7	7.58	–	–	7.58	.17	10.307
4990.509	FeII	–	–	9	–	–	–	7.76	–	.18	10.328
4993.358	FeII	9	6	–	7	7.81	7.58	–	7.62	–3.65	2.806
5001.959	FeII	–	19	–	–	–	7.66	–	–	.90	10.272
5018.440	FeII	55	50	60	50	7.84	7.65	7.94	7.58	–1.22	2.891
5035.708	FeII	–	15	–	13	–	7.72	–	7.60	.61	10.287
5067.893	FeII	–	4.5	–	4	–	7.72	–	7.66	–.20	10.328
5089.214	FeII	4.5	–	–	–	7.56	–	–	–	–.04	10.328
5169.033	FeII	–	55	60	–	–	7.49	7.60	–	–.87	2.891
5197.577	FeII	–	33	29	30	–	7.85	7.56	7.61	–2.10	3.230
5260.259	FeII	–	20	–	–	–	7.67	–	–	1.07	10.418
5264.812	FeII	–	16	–	–	–	8.07	–	–	–3.26	3.230
5276.002	FeII	–	37	32	–	–	7.90	7.56	–	–1.94	3.199
5284.109	FeII	13	–	16	14	7.66	–	7.77	7.67	–3.19	2.891
5291.666	FeII	–	9	–	–	–	7.50	–	–	.57	10.480
5325.553	FeII	–	14	13	–	–	8.00	7.90	–	–3.30	3.221
5408.811	FeII	4	–	–	–	7.76	–	–	–	–2.39	5.956
5465.931	FeII	–	7	–	7	–	7.49	–	7.50	.52	10.622
5529.932	FeII	7	–	–	–	7.96	–	–	–	–1.88	6.729
5534.847	FeII	14	16	16	15	7.66	7.77	7.72	7.67	–2.93	3.245
5643.880	FeII	6	–	–	–	7.93	–	–	–	–1.46	7.653
5645.392	FeII	–	–	6	–	–	–	7.81	–	.09	10.561
5783.630	FeII	5.5	–	–	–	7.75	–	–	–	.21	10.714
5835.492	FeII	–	4	–	3.5	–	7.76	–	7.67	–2.37	5.911
5871.799	FeII	–	–	3	–	–	–	7.69	–	.02	10.828
5991.376	FeII	5.5	7	4	6	7.68	7.82	7.47	7.68	–3.56	3.153
6147.741	FeII	11	10	10	12	7.67	7.60	7.56	7.68	–2.72	3.888
6149.258	FeII	13	9	9	11	7.91	7.66	7.62	7.75	–2.85	3.889
6175.146	FeII	6	7	7	5	7.78	7.87	7.85	7.66	–1.98	6.222
6238.392	FeII	–	12	13	14	–	7.64	7.66	7.71	–2.63	3.888

Table 3. (Contd.)

λ, Å	Ion	Equivalent width, mA				log*N* (log*N*(H) = 12.00)				log*gf*	*Ei*
		component A		component B		component A		component B			
		1	2	1	2	1	2	1	2		
6247.557	FeII	22	20	–	18	7.90	7.79	–	7.64	2.33	3.891
6305.296	FeII	4	–	–	–	7.63	–	–	–	–2.04	6.218
6317.983	FeII	13	11	–	8	7.95	7.8	–	7.58	–1.99	5.510
6331.954	FeII	–	–	–	5	–	–	–	7.68	–1.98	6.217
6383.722	FeII	–	–	6	–	–	–	7.70	–	–2.25	5.552
6416.919	FeII	10	9	9	10	7.72	7.6	7.61	7.68	–2.82	3.891
4714.408	NiI	–	–	3	–	–	–	6.62	–	.23	3.380
4722.153	ZnI	–	–	5	–	–	–	5.89	–	–.34	4.029
4883.684	YII	–	–	32	31	–	–	4.99	4.92	.07	1.084
5087.416	YII	–	–	35	35	–	–	5.45	5.45	–.17	1.084
5200.406	YII	–	–	–	34	–	–	–	5.72	–.57	.992
5205.724	YII	–	–	27	29	–	–	5.01	5.16	–.34	1.032
5402.774	YII	–	–	24	26	–	–	5.43	5.56	–.51	1.839
5473.388	YII	–	–	13	11	–	–	5.18	5.06	–1.02	1.738
5497.408	YII	–	–	–	26	–	–	–	5.59	–.58	1.748
5728.890	YII	–	–	6	–	–	–	4.85	–	–1.12	1.839
5781.689	YII	–	–	6	–	–	–	4.64	–	–.91	1.839
4443.008	ZrII	–	–	12	–	–	–	4.41	–	–.33	1.486
4496.980	ZrII	–	–	5	7	–	–	3.98	4.17	–.86	.713
4554.029	BaII*	10	–	22	24	3.50	–	3.95	3.92	.17	.000
4934.076	BaII*	8	10	16	17	3.38	3.43	3.78	3.69	–.15	.000
6141.713	BaII*	–	5	–	12	–	3.33	–	3.62	–.08	.704
6496.897	BaII*	–	–	–	21	–	–	–	3.96	–.38	.604
4655.480	LaII	–	–	3	3	–	–	4.05	4.05	.07	1.946
4460.207	CeII	–	–	4	–	–	–	3.95	–	.17	.478
5335.159	YbII	–	–	14	–	–	–	4.54	–	.11	3.789
5352.954	YbII	–	–	8	9	–	–	4.15	4.23	.01	3.747
5837.136	YbII	–	–	4	–	–	–	4.35	–	–.44	4.013
6644.582	HfII	–	–	–	3	–	–	–	4.37	–1.55	1.780
4658.283	WII	–	–	–	4	–	–	–	4.29	–.78	2.907
4959.369	WII	–	–	–	4	–	–	–	4.45	–1.02	2.745
5104.432	WII	–	–	–	3	–	–	–	3.99	–.91	2.354
5353.699	WII	–	–	–	4	–	–	–	4.64	–1.30	2.536
4498.678	PtI	–	–	–	4	–	–	–	6.29	.17	3.739
4520.888	PtI	–	–	3	3.5	–	–	6.65	6.73	.16	4.683
5475.767	PtI	–	–	6	–	–	–	6.81	–	.18	4.230
5840.126	PtI	–	–	4	–	–	–	7.27	–	–1.76	1.922
5837.374	AuI	–	–	5	–	–	–	6.66	–	–.57	4.632
5460.731	HgI	–	–	5	3.5	–	–	5.98	5.78	–.14	5.460
6149.873	HgII	–	–	3	–	–	–	6.40	–	.33	11.866

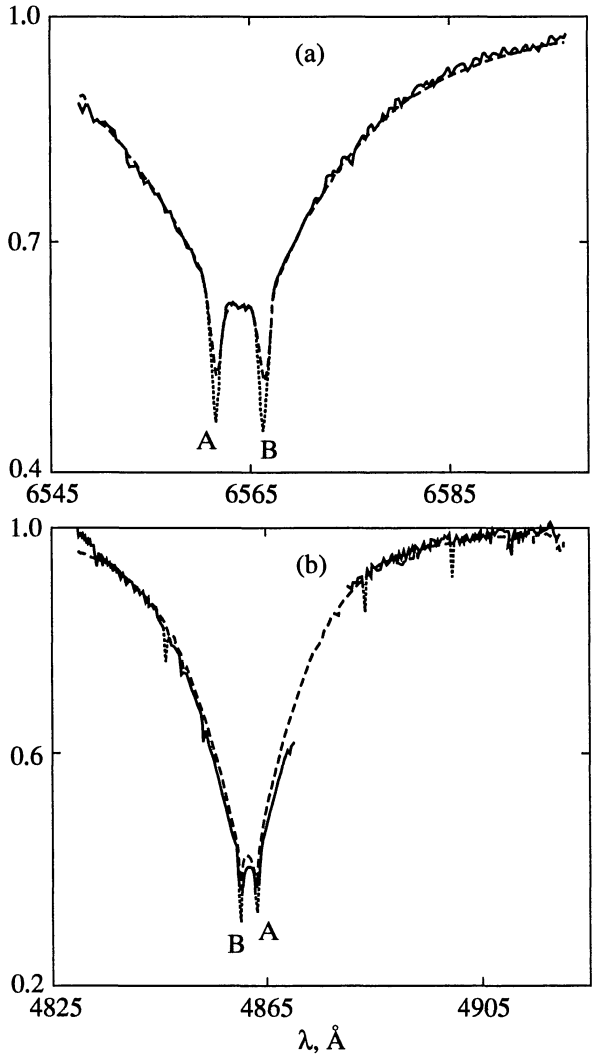

Fig. 4. Comparison of the observed (solid lines) and computed (dashed lines) hydrogen-line profiles in the spectrum of 66 Eri: (a) the first phase, Hα; and (b) the second phase, Hβ.

there is no synchronization and the rotation period of the components is approximately 7.5 days, i.e., close to that found by Schneider (1987). Recall, however, that our analysis of the Hipparcos data revealed no such period.

Thus, the question of synchronization and coaxiality of the rotation and orbital motion of 66 Eri remains an open question. Assuming that they take place, we face the need to explain the small component radii.

ATMOSPHERIC CHEMICAL COMPOSITION OF THE COMPONENTS OF 66 ERI

In order to identify lines in the spectrum of 66 Eri, we computed a synthetic spectrum for each component in the wavelength range 4385–6695 Å. For the calculations, we used a modified version of the code for computing synthetic spectra by Tsymbal (1994) and the line lists of Kurucz (1993) from the eighteenth and twenty-third CD-ROMs. To construct a combined spectrum of the binary system, the synthetic spectra of the components were shifted in accordance with the observed radial velocities and added up with allowance for the relative brightness of the components.

Figure 5 shows portions of the spectrum of 66 Eri; they are fitted by the sum of synthetic spectra for the two components.

To determine the abundances, we selected only lines that were free from blending with lines in the spectra of both components at the epoch of observation. The abundances of the elements with atomic numbers $Z > 16$, except for barium, were determined by the model-atmosphere method. We used the WIDTH9 code (Kurucz 1993) to compute the abundances. The He, C, N, Ne, Mg, Al, Si, and Ba abundances were determined by the synthetic-spectrum method. For barium, we took into account the hyperfine structure of its lines; the data were taken from Francois (1996). We used the SYNTHE code for computing synthetic spectra (Kurucz 1993). The observed spectrum was automatically fitted with a synthetic spectrum by using the URAN software package (Yushchenko 1998), which allows the oscillator strengths of spectral lines to be varied until the desired quality of the fit is achieved. Examples of similar codes were described by Cowley (1995, 1996) and Valenti and Piskunov (1996).

The full list of lines used to determine the abundances is given in Table 3. This table gives the wavelengths and identifications of lines, the equivalent widths of these lines in the spectra of components A and B on our two spectrograms, the abundance derived from a given line, the oscillator strengths, and the energies of the lower level for the lines. In most cases, the oscillator strengths of the lines matched their values recommended in the VALD database (Piskunov *et al.* 1995). For several lines, we used solar oscillator strengths (Gurtovenko and Kostyk 1989). For the lines that were reduced by the synthetic-spectrum method, the equivalent width are given as an illustration only. These lines are marked by asterisks.

We attempted to identify the lines of P, Ga, and Xe but could not find any lines of these elements in the spectra of both components.

The mean results for each element are collected in Table 4. For the two components of 66 Eri and for each element studied, this table gives the total number of lines of this element (ion) in the two observed spectra (n), its mean abundance on the scale $\log N(\mathrm{H}) = 12$, the rms error of a single measurement (σ), and the atmospheric abundance of the element in components A and B relative to its solar value (A–⊙ or B–⊙). The solar atmospheric abundances were taken from Grevesse and Noels (1993).

For components A and B, we determined the abundances of 15 and 26 elements, respectively. The atmospheric chemical composition of the components of

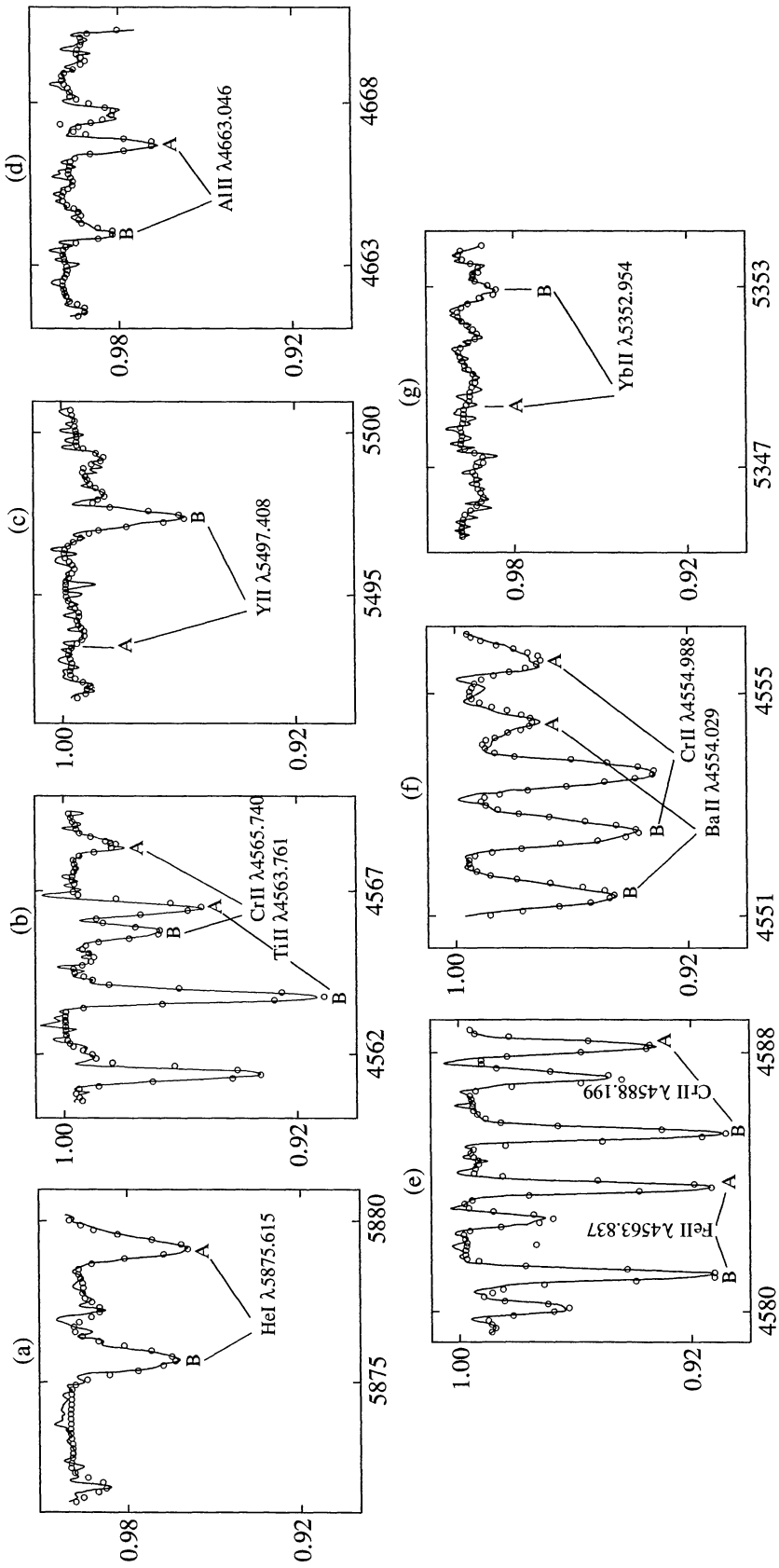

Fig. 5 Portions of the spectrum of 66 Eri fitted by the sum of synthetic spectra for the components. The positions of the helium (a), titanium (b), yttrium (c), aluminum (d), chromium and iron (e), barium (f), and ytterbium (g) lines attributable to the contributions of components A and B are marked.

Table 4. Atmospheric abundances in the components of 66 Eri

z	Ion	A		σ	B		σ	A–⊙	B–⊙
		n	log$N$		n	log$N$			
2	HeI	6	10.98	.09	5	10.98	.03	–.01	–.01
6	CI	1	8.40		1	8.37		–.16	–.19
8	OI	9	8.79	.03	7	8.68	.01	–.14	–.25
10	NeI	1	8.15					.06	
12	MgI	6	7.49	.07	5	7.15	.07	–.09	–.43
	MgII	6	7.49	.17	5	7.28	.13	–.09	–.30
13	AlII	4	6.64	.09	2	6.32	.11	.17	–.15
14	SiII	7	6.97	.19	5	6.87	.07	–.58	–.68
16	SII	2	7.34	.13	1	7.26		.13	.05
20	CaII	2	6.50	.04	2	6.24	.01	.14	–.12
21	ScII	1	3.35		1	3.14		.25	.04
22	TiII	22	5.21	.15	27	5.91	.21	.22	.92
24	CrI				1	6.09			.41
	CrII	20	5.84	.18	18	6.34	.14	.17	.67
25	MnII	2	6.00	.18	3	6.39	.20	.61	1.01
26	FeI	7	7.79	.05	8	7.55	.14	.15	–.09
	FeII	62	7.72	.13	60	7.66	.10	.08	.02
28	NiI				1	6.62			.37
30	ZnI				1	5.89			1.29
39	YII				14	5.21	.31		2.97
40	ZrII				3	4.19	.17		1.59
56	BaII	4	3.41	.06	6	3.82	.13	1.28	1.69
57	LaII				2	4.05			2.83
58	CeII				1	3.95			2.40
70	YbII				4	4.32	.15		3.24
72	HfII				1	4.37			3.49
74	WII				4	4.34	.24		3.23
78	PtI				5	6.75	.31		4.95
79	AuI				1	6.66			5.65
80	HgI				2	5.88	.10		4.79
	HgII				1	6.40			5.31

66 Eri is shown in Fig. 6. We see from this figure that there are large differences in the atmospheric abundances of titanium, chromium, manganese, and heavy elements between the components of 66 Eri.

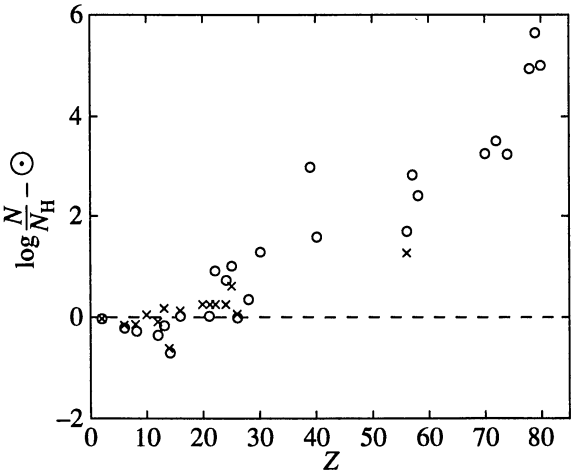

Fig. 6. Atmospheric chemical composition of the components of 66 Eri relative to the Sun: the crosses and circles are for components A and B, respectively.

For the elements that were represented by the largest number of lines (Fe, Ti, Mn, Cr), we calculated the correlation coefficients between the Lande factors and the abundances computed from these lines. No appreciable correlation was found.

CONCLUSION

66 Eri is an SB2 system with a component–mass ratio that is closest to unity (and with virtually equal temperatures and effective gravities) among the twin stars of our program (AR Aur and 46 Dra) studied to date.

To determine the mean effective temperatures and surface gravities of the components of 66 Eri, we used all available photometric and spectrophotometric observations in a wide wavelength range, which yielded $T_{\rm eff} = 11000$ K and $\log g = 4.25$.

An infrared excess reaching two orders of magnitude shows up at wavelengths longer than 25 μm, suggesting that the system is surrounded by a dust envelope. The binary systems 46 Dra, V686 Cra, and HD 153720,

which we study as part of our program, also exhibit a similar infrared excess.

An analysis of the Hipparcos photometric observations has revealed small light variations with the period equal to half the orbital period and an amplitude ~$0^m.005$ (in the Hipparcos photometric system). This variability can be attributed either to a partial eclipse in 66 Eri, or to irregularity of the surface of the peculiar component, or to a small ellipticity of the components. One of these alternatives or their combination can be chosen only after new high-accuracy photometric observations of 66 Eri are obtained.

Our rotational velocity of the components $v \sin i$ = 17 km s^{-1}, the Hipparcos parallax of the binary system, and a frequency analysis of the Hipparcos photometric observations of 66 Eri suggest that the rotation of the components is synchronized with the orbital period.

The spectroscopic observations of 66 Eri allowed us to determine the temperature and microturbulent velocity for each component and the component–luminosity ratio:

$$T_{\mathrm{eff_A}} = 11\,100 \pm 100\ \mathrm{K},\ V_{\mathrm{turb_A}} = 0.9 \pm 0.2\ \mathrm{km\ s^{-1}},$$

$$T_{\mathrm{eff_B}} = 10\,100 \pm 100\ \mathrm{K},\ V_{\mathrm{turb_B}} = 0.7 \pm 0.2\ \mathrm{km\ s^{-1}},$$

$$L_A/L_B = 0.95 \pm 0.05.$$

The components were found to differ in chemical composition. Component B, which has been previously classified as an Hg–Mn star, exhibits no anomalies typical of this type of star, such as an underabundance of helium and aluminum and an overabundance of phosphorous and gallium. Large heavy-element overabundances reaching 4–5 dex are observed in component B. Note that heavy elements are enhanced in the atmospheres of magnetic CP stars, in particular, in their prototype α^2 CVn. However, the search for a correlation of the Fe, Ti, Mn, and Cr abundances with the Lande factors of the lines yielded a negative result.

Component A exhibits moderate overabundances of Mn and Ba. No lines of heavy elements, except for barium, were found in its spectrum. We computed a synthetic spectrum for component A with overabundances of heavy elements reaching 1.5–2 dex and made sure that the intensities of the heavy-element lines for this case were below the detection threshold. Estimates of the upper limit on the heavy-element abundances show that a heavy-element overabundance in the atmosphere of component A cannot be completely ruled out either.

66 Eri is the first binary among the SB2 systems studied to date with late B-type, chemically peculiar non-Hg–Mn components.

ACKNOWLEDGMENTS

We wish to thank G.A. Galazutdinov for help in the observations and for providing a new version of the DECH software package. We used the NASA ADS bibliographic database. This study was supported in part by the Russian State Science and Technology Program "Astronomy."

REFERENCES

Allen, C., *Astrophysical Quantities*, London: The Athlone, 1973. Translated under the title *Astrofizicheskie velichiny*, Moscow: Mir, 1977.

Andronov, I.L., *Odessa Astron. Publ.*, 1994, vol. 7, p. 49.

Batten, A.H., Fletcher, J.M., and McCarthy, D.C., Eighth Catalogue of the Orbital Elements of Spectroscopic Binary Systems, *Publ. Dom. Astrophys. Obs.*, 1989, vol. 17, p. 1.

Berghofer, T.W. and Schmidt, J.H.M.M., *Astron. Astrophys.*, 1994, vol. 292, p. L5.

Cowley, C.R., Laboratory and Astronomical High Resolution Spectra, *ASP Conf. Ser.*, Sauval, A.J. *et al.*, Eds., 1995, vol. 81, p. 467.

Cowley, C.R., Model Atmospheres and Spectrum Synthesis, *ASP Conf. Ser.*, Adelman, S.J. *et al.*, Eds., 1996, vol. 108, p. 170.

Dimming, T.J., *Astrophys. Space Sci.*, 1975, vol. 36, p. 147.

Dougherty, S.M., Cramer, N., Van Kerkwijk, M.H., *et al.*, *Astron. Astrophys.*, 1993, vol. 273, p. 503.

Francois, P., *Astron. Astrophys.*, 1996, vol. 313, p. 229.

Frost, E.B. and Struve, O., *Astrophys. J.*, 1924, vol. 60, p. 313.

Galazutdinov, G.A, *Preprint of Spets. Astrofiz. Obs. Ross. Akad. Nauk*, 1992, no. 92.

Gezari, D.Y., Pitts, P.S., Schmitz, M., and Mead, J.M., *Catalog of Infrared Observations*, ed. 3.5, 1996 (ADS CD-ROM 3).

Grevesse, N. and Noels, R., *Origin and Evolution of the Elements*, Prantzos, N. *et al.*, Eds., Cambridge: Cambridge Univ., 1993, p. 15.

Gurtovenko, E.A. and Kostyk, R.I., *Fraungoferov spektr i sistema solnechnykh sil ostsillyatorov* (The Fraunhofer Spectrum and a Set of Oscillator Strengths), Kiev: Naukova Dumka, 1989.

Hauck, B. and Mermilliod, M., *Astron. Astrophys., Suppl. Ser.*, 1990, vol. 86, p. 107.

Jamar, C., Macau-Hercot, D., Monfils, A., *et al.*, *Ultraviolet Bright-Star Spectrophotometric Catalogue*, ESA, 1976, (ADC CD-ROM 1, 1991).

Kasatella, A., *Astron. Astrophys.*, 1975, vol. 48, p. 281.

Khokhlova, V.L., Zverko, Yu., Ziznovsky, J., *et al.*, *Pis'ma Astron. Zh.*, 1995, vol. 21, p. 908. *Astron. Lett.*, 1995, vol. 21. p. 818.

Kunzli, M., North, P., Kurucz, R.L., and Nicolet, B., *Astron. Astrophys., Suppl. Ser.*, 1997, vol. 122, p. 51.

Kurucz, R.L., *CD-ROMs 1-23*, Smithson. Astrophys. Obs., 1993.

Lanz, T., *Astron. Astrophys., Suppl. Ser.*, 1986, vol. 65, p. 195.

Moshir, M., Kopan, G., Conrow, T., *et al.*, *The IRAS Faint Source Survey, Version 2.0*, 1989 (ADC CD-ROM 1, 1991).

Musaev, F.A., *Pis'ma Astron. Zh.*, 1996, vol. 22, p. 795. *Astron. Lett.*, 1996, vol. 22. p. 715.

Perryman, V.A.C., *The Hipparcos and Tycho Catalogues*, European Space Agency (CD-ROMs 1–8, 1997).

Piskunov, N.E., Kupka, F., Ryabchikova, T.A., *et al.*, *Astron. Astrophys.*, 1995, vol. 301, p. 951.

Rufener, F., *Catalogue of Stars Measured in the Geneva Observatory Photometric System, 4th Edition*, Geneva: Observatoire de Geneve, 1988 (ADC CD-ROM 1, 1991).

Schneider, H., *Hvar. Obs. Bull.*, 1987, vol. 11, p. 29.

Smalley, B., Model Atmospheres and Stellar Spectra, *ASP Conf. Ser.*, Adelman, S.J. and Weiss, W.W., Eds., 1996, vol. 108, p. 198.

Stepien, K., *Chemically Peculiar and Magnetic Stars*, Zverko, J. and Ziznovsky, J., Eds., Tatranska Lomnica, 1994, p. 8.

Thompson, G.I., Nandy, K., Jamar, C., *et al.*, *Catalogue of Stellar Ultraviolet Fluxes*, The Science Research Council, 1978 (ADC CD-ROM 1, 1991).

Tsymbal, V.V., *Model Atmospheres and Stellar Spectra*, Adelman, S.J. and Weiss, W.W., Eds., 1996, vol. 108, p. 198.

Tsymbal, V.V., *Odessa Astron. Publ.*, 1994, vol. 7, p. 146.

Tsymbal, V.V., Kotchukhov, O.P., Khokhlova, V.L., and Lambert, D.L., *Pis'ma Astron. Zh.*, 1998, vol. 24, p. 116. *Astron. Lett.*, 1998, vol. 24. p. 90.

Valenti, J.A. and Piskunov, N.E., Model Atmospheres and Spectrum Synthesis, *ASP Conf. Ser.*, Adelman, S.J. *et al.*, Eds., 1996, vol. 108, p. 175.

Wesselius, P.R., van Duinen, R.J., de Jonge, A.R.W., *et al.*, *Astron. Astrophys., Suppl. Ser.*, 1982, vol. 49, p. 427.

Young, A., *Publ. Astron. Soc. Pac.*, 1976, vol. 88, p. 275.

Yushchenko, A.V., *Proc. 29th Conf. Variable Star Research*, Dusek, J. and Zejda, M., Eds., Brno, 1998, p. 202.

Yushchenko, A.V., Gopka, V.F., Khokhlova, V.L., *et al.*, *Contrib. Astron. Obs. Scalnate Pleso*, 1998, vol. 27, p. 365.

Translated by V. Astakhov